Effects of the downsampling scheme on three-dimensional electron microscopy of single particles

C.O.S. Sorzano, A. Iriarte, R. Marabini, J.M. Carazo
Biocomputing Unit
National Center of Biotechnology (CSIC)
c/Darwin,3 Campus Univ. Autnoma, Cantoblanco, Madrid, Spain
coss,ana,roberto,carazo@cnb.csic.es

***Abstract*— Electron microscopy of single particles aims at the elucidation of the three-dimensional structure of macromolecular complexes. This information is crucial for the more complete understanding of how these nanomachines perform their functions in the cell. Electron microscopy images are recorded in digital form at a resolution much higher than needed from the signal theory point of view. Then, they are downsampled to the required resolution. The electron microscopy community has paid little attention to this step assuming that even a trivial filter, as "bining", does not affect the posterior image processing steps. In this paper we show that this hypothesis is not correct.**

I. Introduction

Electron microscopy of macromolecular complexes has been shown to be one of the most powerful techniques to elucidate their three-dimensional structure in nearly native conditions [1]. The process starts by acquiring micrographs of the specimen under study, usually several projections of the specimen are visible in the same micrograph. All these projections come from different macromolecules which are supposed to be identical, although they differ in their relative orientation with respect to the electron beam. After collecting thousands of such projections, they are aligned and reconstructed recovering in this way a three-dimensional structure compatible with the bidimensional projections collected in the micrographs.

Usually, micrographs are digitized between 1 and 2 Å per pixel. However, the final resolution achieved in the 3D reconstruction are in the range between 1/6 and 1/20 $Å^{-1}$, meaning that the original micrographs are much more finely sampled than needed. In order to reduce noise as well as storage space and computation time, micrographs are usually downsampled by a factor of 2 or 3, so that the Nyquist frequency of the downsampled micrographs is more in agreement with the final resolution.

This need for downsampling is widely recognized in the Three-Dimensional Electron Microscopy (3DEM) community, and the most widely used software packages for image processing in this field (SPIDER [2], EMAN [3], IMAGIC [4], and Xmipp [5]) provide programs to perform the downsampling of micrographs. Interestingly, many image procesing protocols have as default option the so-called "binning" downsampling, which is no more than a rectangular pulse antialiasing filter (i.e., for a downsampling by 2, the pixel values of small patches of 2x2 pixels are averaged to produce a single pixel value in the downsampled image). Different arguments have been given to justify the use of binning in downsampling. From a theoretical point of view, the use of this filter is considered "optimal" because it is zero-valued at those right frequencies (those related with the sampling rate). In the practical side, it has been claimed that it does not noticeably affect any of the subsequent image processing steps (personal communication with some of the authors of the aforementioned packages). In this short paper we show that none of the two arguments is valid both from a theoretical point of view (which is widely known to the signal processing community but it is interesting to briefly review here) and from a practical point of view with a number of experiments carried out with images of human adenovirus type 5.

II. Downsampling in theory

The filters actually used for image downsampling are the products of two orthogonal 1D filters along X and Y directions. However, for the sake of simplicity, our discussion will focus on the 1D filters involved, since the generalization to the two-dimensional case is trivial. The Fourier transform of the 1D binning filter with N samples is

$$H(e^{j\omega}) = \frac{1}{N}\frac{\sin\left(\frac{N\omega}{2}\right)}{\sin\left(\frac{\omega}{2}\right)}e^{-j\frac{N-1}{2}\omega} \quad (1)$$

which has the first zero at $\omega_0 = \frac{2\pi}{N}$. However, after the downsampling we are interested in the frequency band between 0 and $\frac{\pi}{N}$, i.e., the zero is twice at the required maximum bandwidth implying an important potential aliasing (as can be seen in Fig. 2). A second drawback of this antialiasing filter is that the frequency components remaining after the downsampling have been monotonically dampened down to a factor

$$\left|H(e^{j\frac{\pi}{N}})\right| = \frac{1}{N}\frac{1}{\sin\left(\frac{\pi}{2N}\right)} \quad (2)$$

instead of the ideal $\frac{1}{N}$ (for $N = 2$ this damping is 3dB below the ideal value, and for $N = 3$ is 6dB below).

The correct design of the antialiasing filter involves more sophisticated windows. Following [6], we have used a sinc convolved with a Kaiser-Bessel window of order 0

$$h[n] = \frac{1}{N}\text{sinc}\left(\frac{n-M}{N}\right)\frac{I_0\left(\beta\sqrt{1-\left(\frac{n}{M}\right)}\right)}{I_0(\beta)}(u[n]-u[n-M-1]) \quad (3)$$

where I_0 is the modified Bessel function of the first kind and $u[n]$ the step function. The total length of the filter is $2M+1$ (M is calculated below), and β is a parameter that is calculated from the width of the transition band $\Delta\omega$ as follows: first an intermediate parameter A is calculated

$$A = -20\log_{10}(\delta),$$

where δ is the ripple allowed in the resulting low-pass filter, and then

$$M = \left\lceil \frac{A-8}{2.285\Delta\omega} \right\rceil \quad (4)$$

and

$$\beta = \begin{cases} 0.1102(A-8.7) & \text{if } 50 \leq A \\ 0.5842(A-21)^{0.4} + 0.07886(A-21) & \text{if } 21 \leq A < 50 \\ 0 & \text{otherwise} \end{cases} \quad (5)$$

Fig. 1 shows the impulse response of this filter for $\delta = 0.02$ and $\Delta\omega = 0.1$ while Fig. 2 shows the amplitude frequency response of this filter as well as the "binning" approach. Note that the Kaiser windowed sinc has a steepest slope at frequency $\frac{\pi}{N}$, meaning that the attenuation at that frequency will be smaller and that it avoids much better the aliasing of those frequencies beyond $\frac{\pi}{N}$.

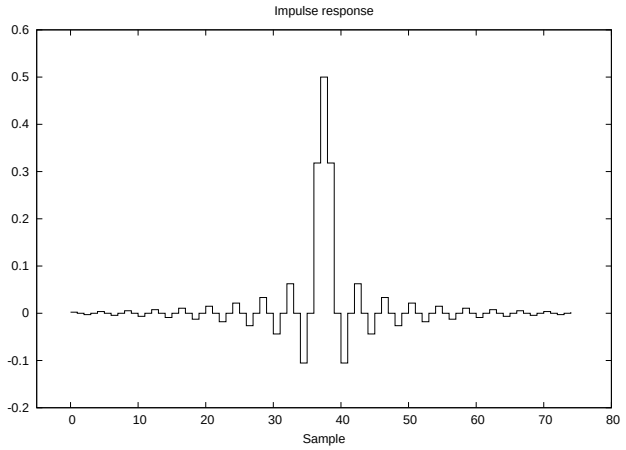

Fig. 1. Impulse response of the Kaiser windowed sinc used as antialiasing filter for $N = 2$.

The main drawback of this filter is that it has a support of about 75 samples. The convolution with such a long filter is certainly time consuming. Alternatively, downsampling can be performed directly in Fourier space by windowing the Fourier transform with a rectangular filter and performing an inverse Fourier transform of the frequencies in the band from 0 to $\frac{\pi}{N}$. Since Fourier transform routines are fast, this is our preferred

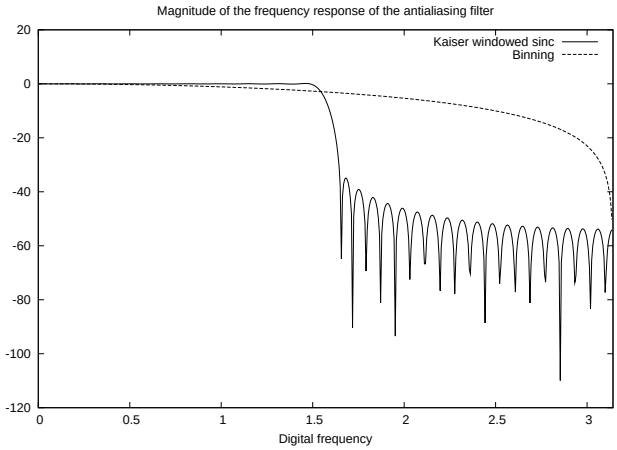

Fig. 2. Amplitude frequency response (in dB) for the binning and the Kaiser windowed sinc. The two frequency responses have been normalized so that at zero frequency both have unit gain.

option and will be referred to as Fourier downsampling. It should be noted at this point that Fourier and sinc based downsampling are equivalent in the continous, so the main difference between the two proposed methos is the windowing with the Kaisser Bessel window.

III. Downsampling in practice

As has already been discussed in the previous section, binning is not the best choice from a theoretical point of view. From a practical point of view, it could be argued that in practice there is no signal at the frequencies in which the aliasing and damping occurs and, consequently, binning or performing a more sophisticated downsampling do not make any difference.

To test this extent we studied a set of 2237 projection images from 129 micrographs of human adenovirus type 5 [7]. Images were recorded on Kodak SO-163 film using a radiation dose of 10 electrons/Å^2, a magnification of 50000x and defocus values in a range between -0.8 and -6μm. Micrographs were digitized in a Zeiss Photoscan TD scanner with a 7μm pixel size (1.4Å in the sample).

The diameter necessary for reconstructing the virus is around 1000Å, which translates in a memory need of 2.7 Gb, thus requiring high-performance computers and a computation time larger than 1 week in a cluster with 64 cores (8 processors, 2 Xeon Quad Core at 2 GHz) to get the 3D reconstruction. However, the resolution achieved in the reconstructed volume reported in [7] was 1/14Å^{-1} meaning that, according to Nyquist theorem, the sampling rate could have been decreased to 7Å per pixel, i.e., a pixel size 5 times larger than the original size. In practice, the pixel size was increased by a downsampling factor 3 [7] (instead of 5), this reduced the computer requirements in 1 order of magnitude.

In our first experiment we performed a Fourier downsampling by a factor 2 (final sampling rate, 2.8Å per pixel) and performed the 3D reconstruction following the projection matching protocol described in [8]. We took a top projection

from the reconstructed volume (note that top projections do not involve any interpolation) and downsampled it by a factor 2 (final sampling rate, 5.6Å per pixel) using Fourier downsampling, the standard downsampling in real space using a Kaiser windowed sinc antialiasing filter ($\delta = 0.02$, $\Delta\omega = 0.1$), and the binning antialiasing filter. The three downsampled projections are shown in Fig. 3. Certainly, the three projections look very similar and this fact may be at the heart of the claim that there is no significant aliasing or dampening of high frequencies. However, we can compare the values of the three projections at a radius of 392Å (close to the border of the capsid). For doing so, we sampled the circumference of that radius every 0.25° at the image with a sampling rate of 2.8Å per pixel, and at the ones at 5.6Å per pixel. Sampling of the circumference was performed using cubic B-splines [9], [10], which have been shown to produce high-quality interpolation. Fig. 4 shows the difference between the sampled values at 2.8Å per pixel and the sampled values of each of the three different downsampling schemes for the first 72° (due to the 5-fold symmetry of the projection, we have represented only the asymetric unit). It can be seen, that there is very little difference between the Fourier and Kaiser windowed sinc schemes. Moreover, the difference between these two profiles at 5.6Å and the values interpolated at 2.8Å is much smaller than the values obtained with the binning scheme. The Signal-to-Noise Ratio (SNR) of the first two schemes are 56.1 dB (Kaiser windowed sinc) and 56.0 dB (Fourier), while the SNR of the binning scheme is 30.3 dB, i.e., there is a difference between the two groups of 26 dB.

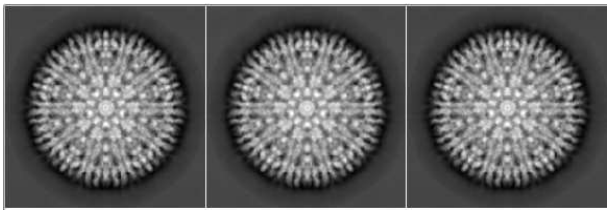

Fig. 3. Top view projections of Adenovirus type 5 at 5.6Å per pixel using three different downsampling schemes: Fourier downsampling (left), real space downsampling with binning antialiasing filter (middle), real space downsampling with Kaiser-sinc antialising filter (right).

It could also be argued that the downsampling is performed at the micrograph level at which the SNR is so low (see Fig. 6) that the downsampling errors are negligible with respect to the image noise level. For testing this extent, we computed the radial averages of the power spectrum densities (PSD) of the micrographs downsampled by a factor 2 (see Fig. 5) using the different downsampling methods (the Fourier and binning downsamplings, both took 4 seconds for a micrograph of 4096x4096 pixels; while the Kaiser windowed sinc took 928 seconds). It can be seen that there is only a small (and expected) difference between Fourier downsampling and real space downsampling with Kaiser windowed sinc antialiasing filter. However, there is a small deviation of the binned micrograph at low frequencies due to the filter damping, and

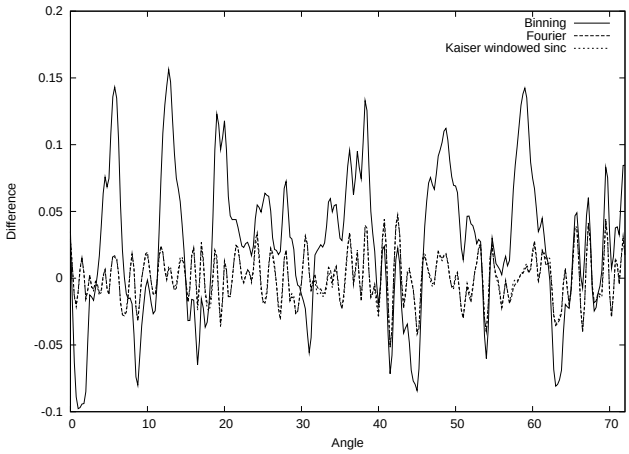

Fig. 4. Difference between the projection at 2.8Å per pixel at a circumference of 392Å and the projections at 5.6Å per pixel with three different downsampling schemes (Binning, Fourier and Kaiser-sinc). Due to the 5-fold symmetry of the values in this circumference, only the first 72° are represented.

a large deviation at high frequencies due to aliasing which is clearly visible in the downsampled micrographs themselves (see Fig. 6).

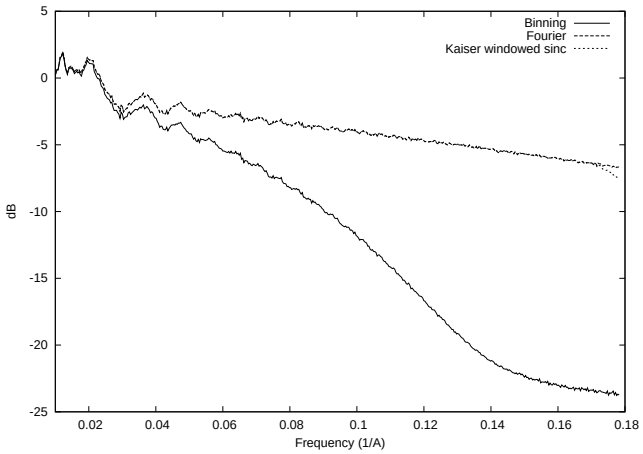

Fig. 5. Radial average of the power spectra of each of the downsampled micrographs

To test how this aliasing influenced subsequent image processing steps, we compared the angular assignment after 13 iterations of the angular projection matching protocol [8] of the images downsampled to 2.8Å per pixel with a Fourier scheme, and the angular assignment for the images downsampled at 4.2Å per pixel with a Fourier scheme, a Kaiser windowed sinc and a binning filter. For each image we compared the angular difference between the Euler coordinate system assigned at 2.8Å and at 4.2Å. We consider that the angular assignment is the same at both resolutions if the average angular difference is smaller than 0.5°. For the Fourier downsampling scheme, the number of images with the same angular assignment was 52.6%, for the Kaiser windowed sinc this proportion decreased to 49.9%, and for the binning scheme was 47.7%

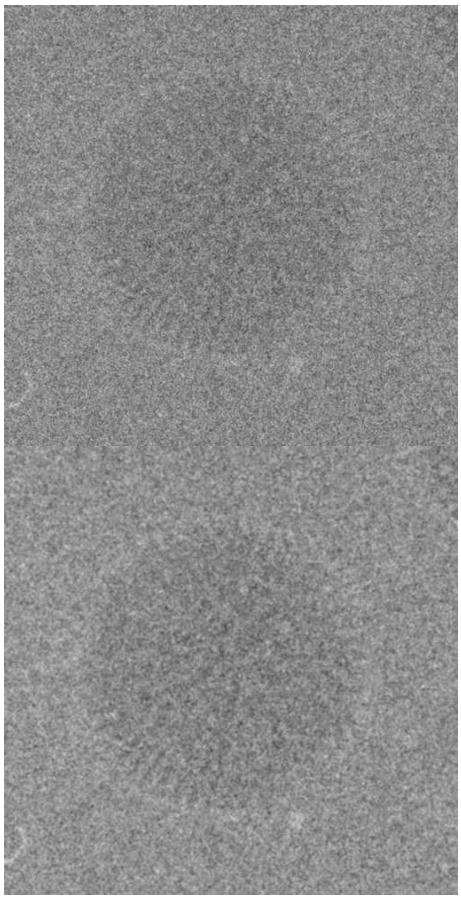

Fig. 6. Top: Micrograph downsampled by a factor 2 using Fourier downsampling. Bottom: Same micrograph using binning downsampling. Note the different texture of the background in both images.

(interestingly, working at a lower resolution strongly affects the angular assigment, the number of images whose angular assignments at high and low resolution coincide drops approximately to 50%). This makes a difference of about 5% between the number of correctly assigned images using the Fourier downsampling scheme and the traditional binning downsampling. This difference was found to be statistically significant with a confidence of 95%. However, the Kaiser windowed sinc was not significantly different to any of the other two schemes at a confidence level of 95%. The reconstructions obtained with Fourier downsampling and binning downsampling do not exhibit any major difference, although it has some fine structure related to the icosahedral capsid instead of just being pure noise (see Fig. 7). However, the Fourier Shell Correlation between these two reconstructions is far from unity (see Fig. 8). The reconstructed volume has a resolution of $1/14\text{Å}^{-1}$. At this frequency the Fourier Shell Correlation between the reconstruction performed with Fourier downsampling and binning downsampling is 0.93 (it is 0.96 for in the case of using Kaiser windowed sinc). The SNR of the reconstructed volume with respect to the noise generated by the downsampling was 26 dB (it was 30dB if the Kaiser windowed sinc is used).

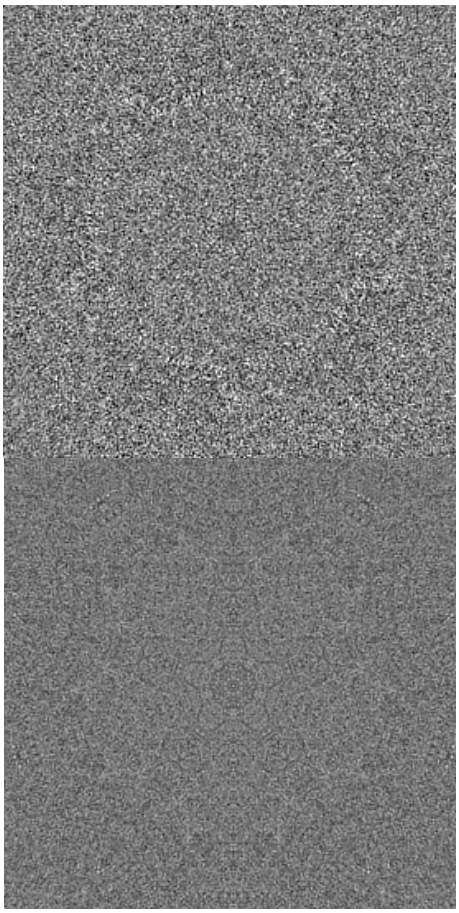

Fig. 7. Top: Central slice of the difference volume reconstructed with Fourier downsampling and binning downsampling. Note the structure of the difference at the location of the capsid. Bottom: Same slice but using the Kaiser windowed sinc. Note that the structured valued are much weaker.

IV. Conclusions

In this paper it has been shown that performing a correct downsampling influences the final result. From a theoretical point of view it is a result already well-known in the signal processing community. From an experimental point of view, it has been shown that aliasing affects the projections from which the 3D structures are computed and the angles assigned to each projection. From these two facts it was hypothesized that the 3D reconstructions would also be affected as has been confirmed by the FSC and the difference volume.

It has been shown that Fourier downsampling is theoretically as well as practically superior to Kaiser windowed sinc convolution and binning. Kaiser windowed sincs are computationally slow due to large size of the kernel used for the convolution in real space. Moreover, it has a small aliasing in a region closed to Nyquist frequency. Binning is computationally very fast, but its results are clearly inferior to the other two methods. Its deffects should not be noticeable if the information content of the image at hand concentrates at very low frequency.

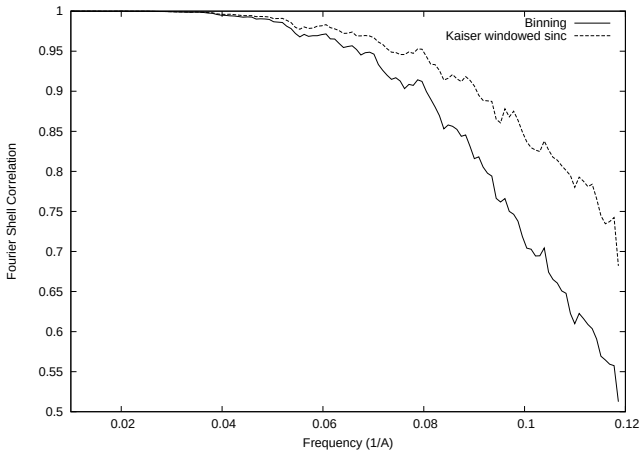

Fig. 8. Fourier Shell Correlation between the volume reconstructed with Fourier downsampling and the one obtained with binning and Kaiser windowed sinc downsampling.

We conclude that performing the right downsampling effectively affects the final 3D reconstruction obtained. However, it should be noted that this effect is not large enough so as to automatically invalidate all structural studies performed by binning the original micrographs. All the downsampling schemes discussed in this paper are freely available from Xmipp [5].

Acknowledgments

This work was funded by the European Union (3DEM Network of excellence FP6-502828 and UE-512092), the Spanish National Council of Scientific Research (CSIC, PIF08-020), the Spanish Ministerio de Ciencia e Innovacin (CSD2006-0023, BIO2007-67150-C01, BIO2007-67150-C03, and BFU2007-60228), the Spanish Fondo de Investigaciones Sanitarias (04/0683), the Universidad San Pablo CEU (USP-PPC 04/07), and the Comunidad Autnoma de Madrid (S-GEN-0166-2006, CCG08-CSIC/SAL-3442) and by Award Number R01HL070472 from the National Heart, Lung, And Blood Institute. The content is solely the responsibility of the authors and does not necessarily represent the official views of the National Heart, Lung, And Blood Institute or the National Institutes of Health.

REFERENCES

[1] J. Frank, *Three-Dimensional Electron Microscopy of Macromolecular Assemblies: Visualization of Biological Molecules in Their Native State*, Oxford Univ. Press, New York, USA, 2006.

[2] J. Frank, M. Radermacher, P. Penczek, J. Zhu, Y. Li, M. Ladjadj, and A. Leith, "SPIDER and WEB: Processing and visualization of images in 3D electron microscopy and related fields.," *J. Structural Biology*, vol. 116, pp. 190–9, 1996.

[3] S. J. Ludtke, P. R. Baldwin, and W. Chiu, "EMAN: Semiautomated software for high-resolution single-particle reconstructions," *J. Structural Biology*, vol. 128, pp. 82–97, 1999.

[4] M. van Heel, G. Harauz, E. V. Orlova, R. Schmidt, and M. Schatz, "A new generation of the IMAGIC image processing system," *J. Structural Biology*, vol. 116, pp. 17–24, 1996.

[5] C. O. S. Sorzano, R. Marabini, , J. Velzquez-Muriel, J. R. Bilbao-Castro, S. H. W. Scheres, J. M. Carazo, and A. Pascual-Montano, "XMIPP: A new generation of an open-source image processing package for electron microscopy," *J. Structural Biology*, vol. 148, pp. 194–204, 2004.

[6] J. F. Kaiser, "Digital filters," in *System analysis by digital computers*, F. F. Kuo and J. F. Kaiser, Eds., pp. 218–285. John Wiley, 1966.

[7] C. San Martn, J. N. Glasgow, A. Borovjagin, M. S. Beatty, E. A. Kashentseva, D. T. Curiel, R. Marabini, and I. P. Dmitriev, "Localization of the N-terminus of minor coat protein IIIa in the adenovirus capsid.," *J. Molecular Biology*, vol. 383, pp. 923–934, 2008.

[8] S. H. W. Scheres, R. Nez-Ramrez, C. O. S. Sorzano, J. M. Carazo, and R. Marabini, "Image processing for electron microscopy single-particle analysis using xmipp," *Nature Protocols*, vol. 3, pp. 977–990, 2008.

[9] M. Unser, A. Aldroubi, and M. Eden, "B-Spline signal processing: Part I - theory," *IEEE Trans. Signal Processing*, vol. 41, pp. 821–832, 1993.

[10] M. Unser, A. Aldroubi, and M. Eden, "B-Spline signal processing: Part II–Efficient design and applications," *IEEE Trans. Signal Processing*, vol. 41, pp. 834–848, 1993.